SCIPEDIA Revista Internacional de Métodos Numéricos para Cálculo y Diseño en Ingeniería

Revista Internacional Métodos numéricos para cálculo y diseño en ingeniería RIMNI

UNIVERSITAT POLITÈCNICA DE CATALUNYA BARCELONATECH In cooperation with CIMNE

Design and structural analysis for a camber-morphing wing with deformable truss

Shancheng Cao[1], Sihan Zhao[1], Yingge Ni[2], Jin Jiao[2]

1 School of Astronautics, Northwestern Polytechnical University, Xi'an 710072, China

2 School of Aircraft Engineering, Xi'an Aeronautical Institute, Xi'an 710077, China

Abstract

A camber-morphing wing based on a deformable truss is proposed in this paper. And then the structural analysis of the proposed camber-morphing wing is achieved. Compared with the existing concept of camber-morphing wings, the deformation mode of this wing is easier to manufacture and implement in engineering. Due to the fact that the wing is driven by multiple motors, it has the characteristic of multiple degrees of freedom in camber-morphing, which can achieve various deformation controls. Establishing corresponding finite element models, the deformation ability under different driving conditions is simulated. The results indicate that compared with driving short metal wires, driving long metal wires results in a greater degree of trailing edge deflection due to a greater driving force. Based on finite element analysis of deformation capability, the camber-morphing wing exhibits satisfactory deformation capability. Furthermore, based on the analysis of load-bearing capacity, it is indicated that the camber-morphing wing has sufficient load-bearing capacity.

OPEN ACCESS

Published: 03/04/2024

Accepted: 14/03/2024

Submitted: 27/02/2024

DOI: 10.23967/j.rimni.2024.03.004

Keywords:
camber-morphing wing
deformable truss
structural analysis
finite element method

1. Introduction

Changing the aerodynamic shape of the aircraft structure to improve flight performance and multi-task capabilities, achieve fuel consumption, reduce noise and pollutant emissions, has always been a research hotspot in the aviation field [1-3]. As one of the ways to change the aerodynamic shape, wing camber morphing technology has become a focus of attention [4-5].

The traditional method of wing camber morphing technology is achieved through hinged control surfaces, which can lead to excessive local aerodynamic surface curvature, resulting in flow separation and excess drag [6-7]. Wings with smooth surfaces and continuous variable camber have enormous potential in improving aircraft performance and fuel efficiency. After replacing traditional hinged flaps with camber-morphing trailing edges, wind tunnel experiments have shown that the lift to drag ratio of the wing will increase by 20% -25% [8-10]. In the Active Compliant Trailing Edge (ACTE) project, full-size distributed flexible seamless deformation trailing edge flaps were utilized to improve aerodynamic efficiency and reduce surrounding noise during takeoff and landing, achieving a deflection angle of -2 ° to +30 ° at a speed of 630 km/h. The test results showed that the deformed flaps significantly improved the flight performance of the carrier aircraft (Gulfstream III test aircraft), reducing cruise resistance by 3%, increasing fuel efficiency by 3% -12%, and reducing noise by 40% [11].

For camber-morphing trailing edge structures, it is necessary to have sufficient flexibility to meet deformation requirements, as well as sufficient stiffness to meet load-bearing capacity requirements [12-13]. Therefore, there are only a few practical designs. For example, the adaptive "rib belt" that replaces traditional wing ribs adopts a distributed flexible structure instead of traditional hinge structure, which has the characteristics of large geometric deformation and high load-bearing capacity [14]. However, adopting distributed flexible structures requires topology optimization algorithms and anisotropic materials for variable stiffness design. With existing conditions, flexible structures are difficult to meet large driving load requirements, and the shape after deformation is difficult to accurately control. Based on the principle of "eccentric beam", the camber-morphing trailing edge is driven by intelligent materials to achieve deformation control in the span and chord directions. When driven at a speed of 75 °/s, a deviation of 25 ° can be achieved within 0.33 seconds [15-19]. However, the camber morphing trailing edge structure designed based on the "eccentric beam" theory is difficult to achieve precise deformation and has poor load-bearing capacity, which has not been applied in engineering [20].

Correspondence: Shancheng Cao (ygni.good@163.com), Yingge Ni (ygni.good@163.com). This is an article distributed under the terms of the Creative Commons BY-NC-SA license

A camber-morphing wing structure is proposed in this paper. The wing is mainly composed of internal deformation trusses, which is fixedly connected to the upper skin of the wing to form a deformation structure, maintaining the wing shape while providing sufficient stiffness to withstand external loads. The number of internal deformation trusses can be adjusted according to the size of the wings, achieving flexible structural adjustments. Multiple motors can provide high driving force and achieve large deformation. The deformation ability of the structure is verified using finite element method. Due to its multiple degrees of freedom, this structure can achieve deformation under various driving conditions. At the same time, a load-bearing capacity analysis is conducted on the wing structure, and it is found that the structure has sufficient stiffness to withstand certain external loads.

2. Structural scheme of camber-morphing wing

The entire chord length of the airfoil is 600mm, and the camber-morphing trailing edge accounts for two-thirds of the entire chord, which is 400mm. The width of the structure is set at 300mm. The NACA4418 airfoil is selected as the basic reference airfoil because the driving system of the camber-morphing wing must be supported by a deformable structure. The NACA4418 airfoil has a relatively thick thickness and a smooth lower surface, which is conducive to the installation of the driving system. The schematic diagram of the camber-morphing wing is shown in Figure 1.

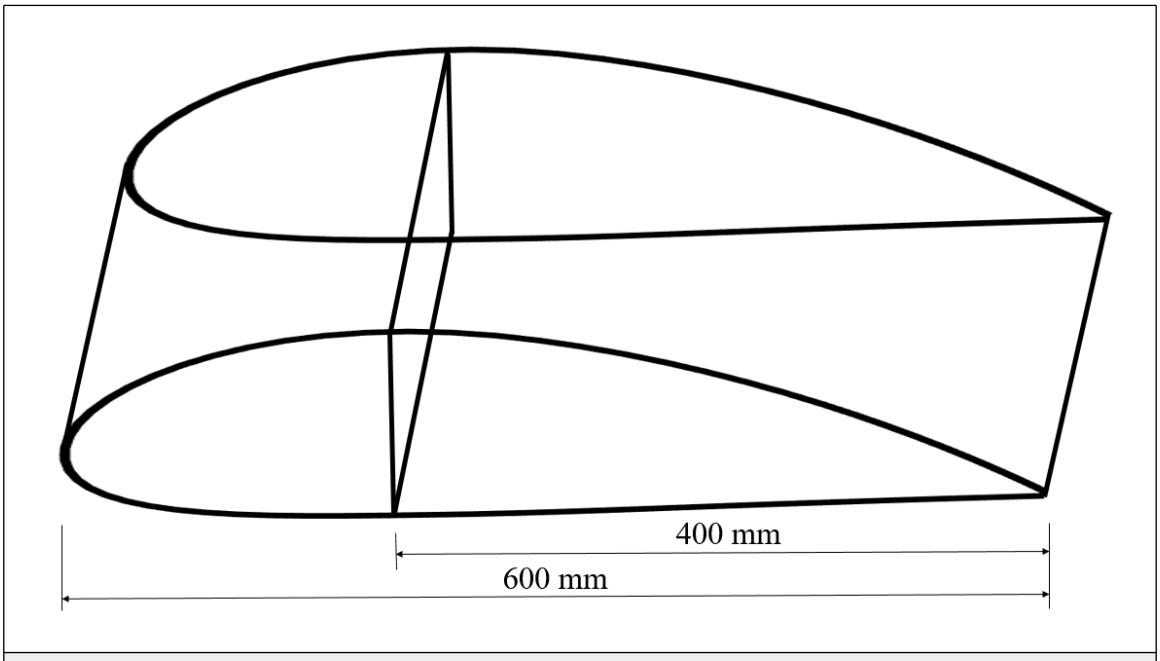

Figure 1. Schematic diagram of camber-morphing wing

The main components of the camber-morphing wing proposed in this paper are the skin, independent deformable truss, and rigid wingtip, as shown in Figure 2. The number of deformable trusses here can be adjusted according to the size of the camber-morphing wing structure, achieving flexible structural adjustment. Firstly, when the motor in the leading edge of the wing acts on the metal wire, the wire can slide to the left, driving the wingtip, thereby extending the upper skin and shrinking the lower skin, achieving continuous and smooth downward deflection of the wing. The deformable truss can not only maintain the wing shape, but also maintain the horizontal deformation of the metal wire. The deformation scheme is more reliable and easy to implement. At the same time, multiple actuators can fully control multiple degrees of freedom and have the characteristic of multi-degree of freedom in camber deformation, making this structure have higher application value and engineering feasibility.

When selecting three or four deformable trusses, the three-dimensional schematic diagram of the entire camber-morphing wing is shown in Figure 3. The trailing edge of the wing is a deformable component, and the upper skin is bonded to the leading edge, deformable truss, and wing tip respectively. The metal wire is divided into two groups, one is a long metal wire and the other is a short metal wire. One end of the long metal wire is directly bonded to the wing tip. The other end is connected to the motor through a groove on the deformable truss. The end of the short metal wire is bonded to one of the deformation trusses. The other is connected to the motor through a groove on the deformable truss. When the motor acts on the metal wire, the wire can slide to the left, driving the wing tip, thereby extending the upper skin and shrinking the lower skin, achieving continuous and smooth downward deflection of the wing. The truss structure maintains the wing shape while bearing the external loads.

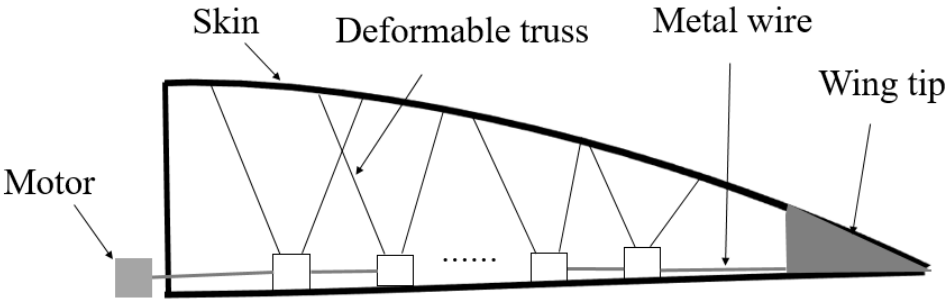

Figure 2. Trailing edge structure of camber-morphing wing

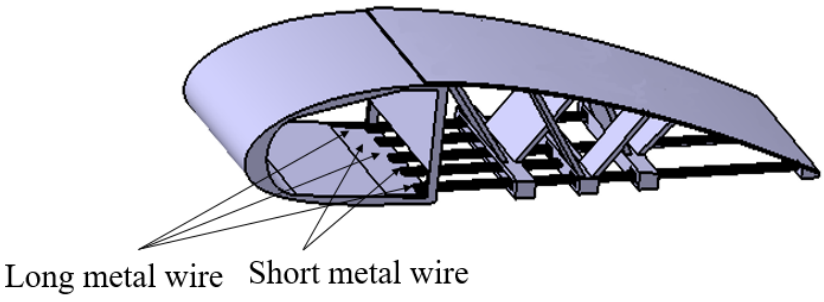

(a) Three deformable trusses

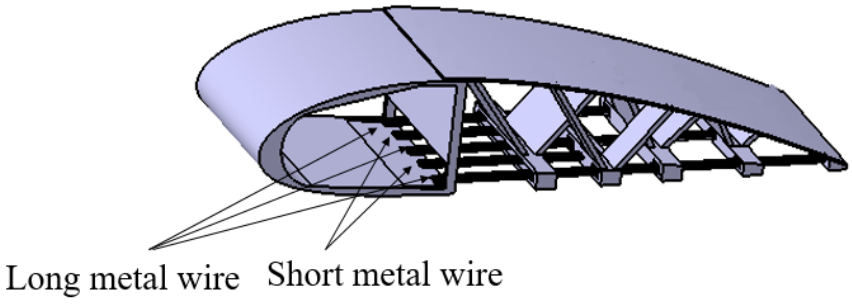

(b) Four deformable trusses

Figure 3. Three dimensional schematic diagram of camber-morphing wing with different numbers of deformable trusses

3. Structural analysis of camber-morphing wing

3.1 Analysis of deformation capacity

The verification of deformation ability aims to use finite element software to simulate the camber-morphing wing model and verify whether the wing can achieve changes in camber with motor.

To achieve changes in the camber, flexible materials should be selected for the skin. The material used in this paper is GRFP, which is glass fiber reinforced material (commonly known as fiberglass). This material has the characteristics of

corrosion resistance, lightweight, and high toughness. The leading edge, deformable truss, and wing tip must withstand stress and deformation, but cannot affect the overall shape of the wing. Therefore, Q235 carbon structural steel is selected. Two sets of short metal wires and three sets of long metal wires are driven and may come contact with the groove after driving, so carbon fiber composite material T300/4211 is selected. The material property data is in Table 1.

Table 1. Material property

Component	Material	Density (t/mm^3)	E (MPa)	Poisson's ratio
Leading edge	Q235 steel	7.85×10^{-9}	206000	0.3
Truss	Q235 steel	7.85×10^{-9}	206000	0.3
Wing tip	Q235 steel	7.85×10^{-9}	206000	0.3
Skin	glass fiber reinforced material GRFP	2×10^{-9}	76000	0.13
Metal wire	carbon fiber T300	1.55×10^{-9}	230000	0.28

To simplify the model, hexahedral elements are used for all components involved in the structure. This makes it easier to achieve mutual coupling and contact between different components. In order to ensure that the metal wires remain horizontal during the pulling process, surface contact is applied between the sliding groove at the bottom of the deformable truss and all the metal wires in the finite element model to ensure that the downward deflection of the wing trailing edge does not cause upward displacement of the metal wires during the simulation process, and to maintain the level as much as possible. In addition, due to the deformation of the truss near the leading edge, there is a sliding groove at the bottom. In the simulation, in order to ensure that the metal wires do not interfere with each other, five reference points are set at the front of each metal, and five metal wires are coupled with five reference points. By applying loads on five reference points, it is ensured that the load is horizontally transmitted to the metal wires, effectively avoiding mutual interference between the metal wires. The final finite element model is shown in Figure 4.

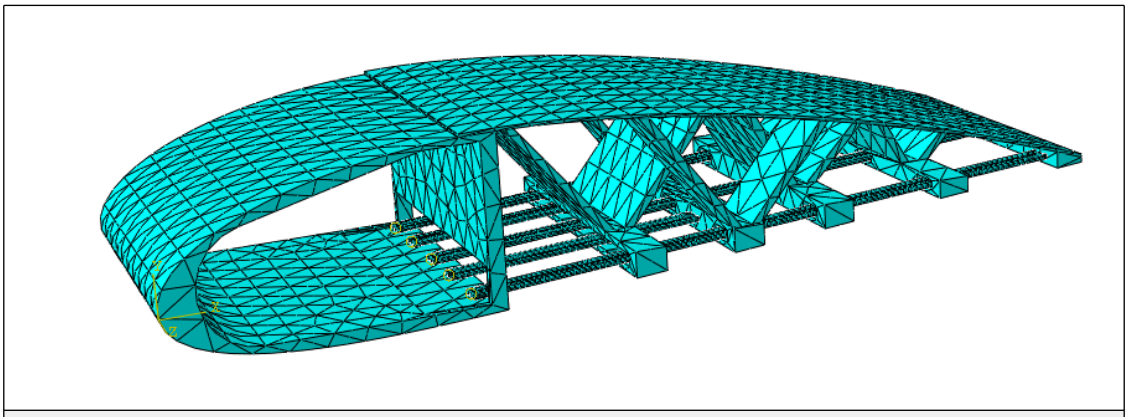

Figure 4. Finite element model for deformation capability analysis

3.1.1 Deformation analysis when driving long metal wires

Firstly, a concentrated force of 500N in the horizontal direction is applied to the end of the three long metal wires, and the corresponding responses are obtained as shown in Figures 5 and 6. From Figure 5, it can be seen that under this driving force, the maximum stress of the camber-morphing wing is 1893MPa, and the maximum stress is concentrated at the contact area between the skin and the first deformable truss. This is because the skin and deformable truss are fixed. When the three sets of metal wires generate horizontal displacement under the driving force, they will drive the entire trailing edge structure to bend downwards. Therefore, there will be stress concentration in the skin at this location. At the same time, when the metal wire passes through the groove of the truss, the truss will also apply pressure to the metal wire, causing slight bending of the metal wire. Therefore, there is also stress concentration in the contact area with the truss.

As shown in Figure 6, when only three long metal wires are driven by the motor, the maximum displacement of the trailing edge of the camber-morphing wing is 73.37mm. Although no concentrated force is applied on the short metal wire, due to the connection between the short metal wire and the deformable truss, the deformable truss will also generate displacement, so there is also displacement of the short metal wire. Due to the downward displacement of

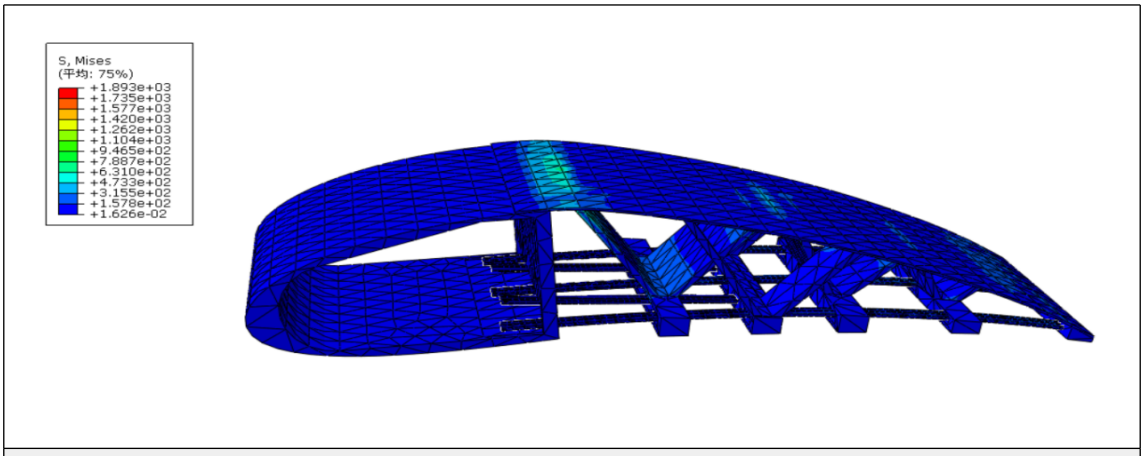

Figure 5. Stress when driving long metal wires

the skin caused by the deformation of the truss, and the downward deflection of each deformable truss is different, the contact between the truss and the metal wire will cause a certain degree of bending of the metal wire. The overall displacement change is consistent with the deformation of the camber-morphing wing model when only pulling the long metal wire.

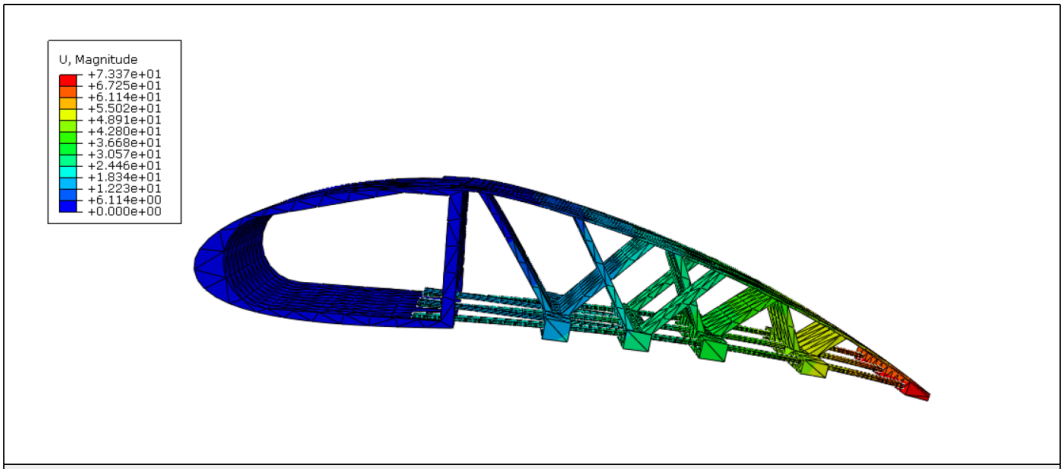

Figure 6. Displacement when driving long metal wires

In order to more intuitively compare the changes in the camber. Figure 7 shows a comparison before and after deformation. Select the outer nodes of the wing as a whole: leading edge, skin and the bottom of trusses (since the wing is not equipped with skin, only the nodes on the truss are selected at the bottom), and generate a comparison diagram of the wing before and after deformation. The maximum downward deviation of the trailing edge is 73.37mm.

3.1.2 Deformation analysis when driving short metal wires

In order to compare the variation of camber under different driving conditions, the driving conditions are changed. Only the short metal wire is pulled, that is, a concentrated force of 500N is applied horizontally on the end of the two sets of short metal wires, and the corresponding response is finally obtained as shown in Figures 8 and 9.

From Figure 8, it can be seen that when only the short metal wire is pulled, stress is generated in all parts of the camber-morphing wing, with a maximum stress of 1288 MPa. The maximum stress is concentrated at the contact area between the leading edge of the front deformable truss and the skin. Due to the deformation of the truss causing downward displacement of the skin, and the downward deflection of each deformable truss is different, the contact between the surface of the groove of the truss and the metal wire will cause a certain degree of bending of the metal

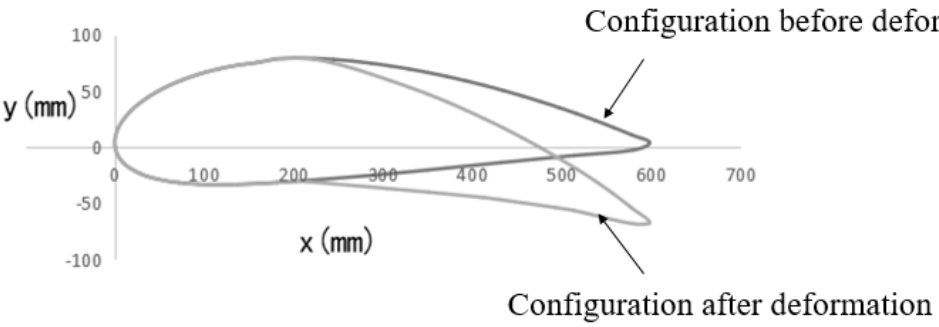

Figure 7. Comparison of configuration before and after deformation when driving long metal wire

wire, resulting in stress concentration at the contact area between the metal wire and the truss.

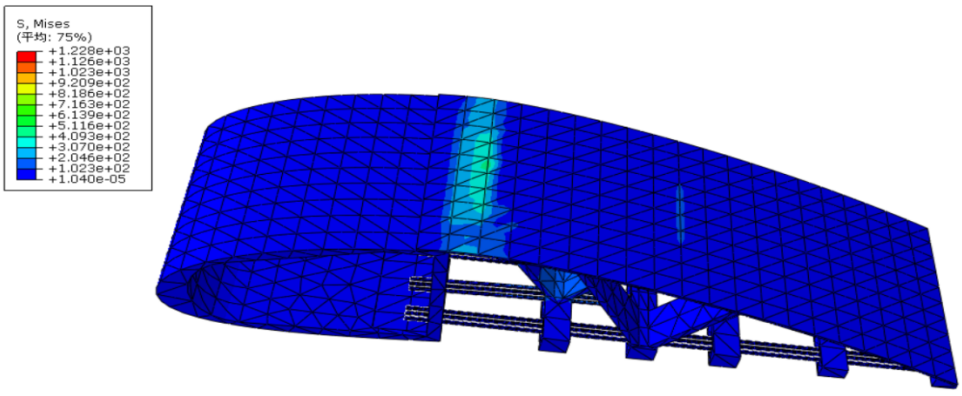

Figure 8. Stress when driving short metal wires

As shown in Figure 9, when only two sets of short metal wires are pulled, the maximum displacement generated by the trailing edge of the camber-morphing wing is 39.38mm. Although no concentrated force is applied to the long metal wire, due to the connection between the long metal wire and the deformable truss, when the short metal wire is pulled, the deformation truss will also generate displacement, so there is also displacement in the short metal wire. Due to the downward displacement of the skin caused by the deformation of the truss, and the downward deflection of each deformable truss is different, the groove of the truss contacts with the metal wire, which will cause a certain degree of bending of the metal wire. The overall displacement change is consistent with the deformation of the camber-morphing wing model when only pulling the short metal wire.

To provide a more intuitive comparison of the camber of the wings, Figure 10 shows a comparison before and after deformation. The outer nodes of the wing as a whole are selected: leading edge, outer skin, and the truss bottom. The trailing edge achieves a maximum downward deviation of 39.38mm.

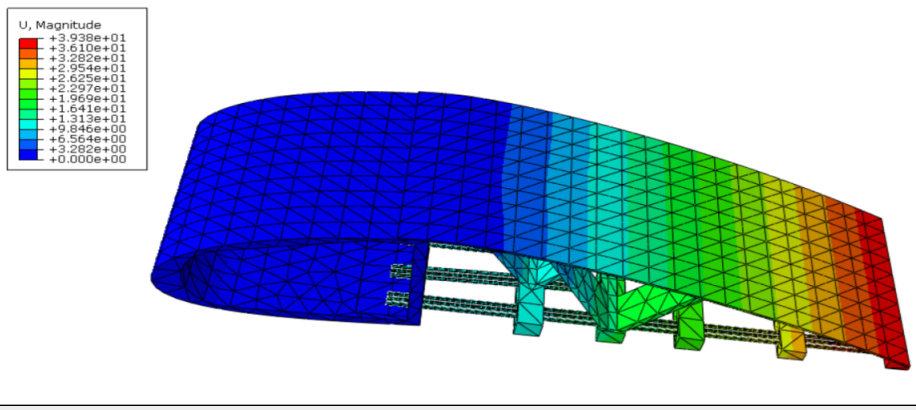

Figure 9. Displacement when driving short metal wires

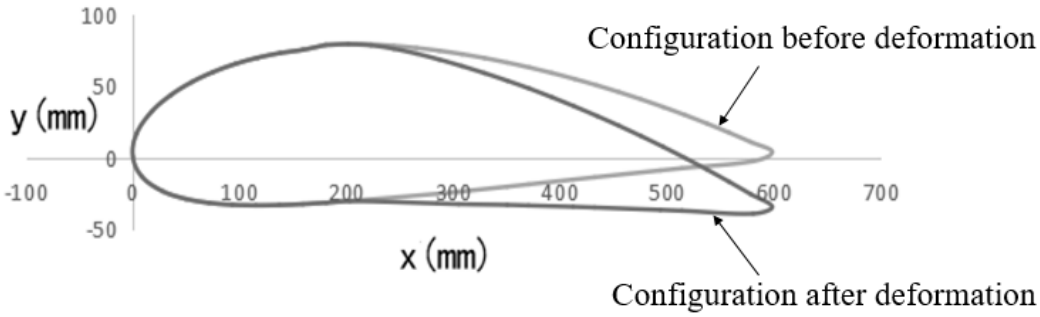

Figure 10. Comparison of configuration before and after deformation when driving short metal wire

Comparing Figures 7 and 10, it can be observed that under the motor, when the long metal wire is pulled, the downward displacement of the wing trailing edge is greater, indicating that the degree of camber is higher when the long metal wire is driven. It further indicates that in order to achieve greater downward displacement of the trailing edge of the wing, both long and short metal wires can be driven simultaneously. This can also be seen from the wing structure scheme: firstly, the resultant force when driving long metal wires is greater than that when driving short metal wires; secondly, when driving a long metal wire, the driving force is directly transmitted along the wire to the wing tip, which is equivalent to the force acting on the wing tip, directly driving the upper skin to achieve downward deflection. When driving a short metal wire, the driving force is transmitted along the short metal wire to the lower edge of the deformable truss, which is equivalent to the force acting on the deformable truss, indirectly driving the upper skin to achieve downward deflection. Therefore, when driving a long metal wire, the degree of camber is higher.

3.2 Load-bearing capacity analysis

Carrying capacity is another goal of morphing wing design, aimed at using finite element software to simulate the camber-morphing wing model and verify whether the wing has sufficient carrying capacity under the external loads.

The finite element model in this section is different from the finite element model in Section 3.1. The main reason is that when conducting load-bearing capacity analysis, the leading edge is fixed, and its load-bearing capacity is mainly reflected by the deformation of the trailing edge. In addition, the number of deformable truss is three to verify whether the structure has sufficient load-bearing capacity when the stiffness of the wing structure decreases. The final finite element model is shown in Figure 11, where the connection between the skin and the leading edge is fully fixed and uniformly distributed pressure is applied to the lower and upper skin of the truss, respectively. Its material properties are the same as those in Section 3.1.

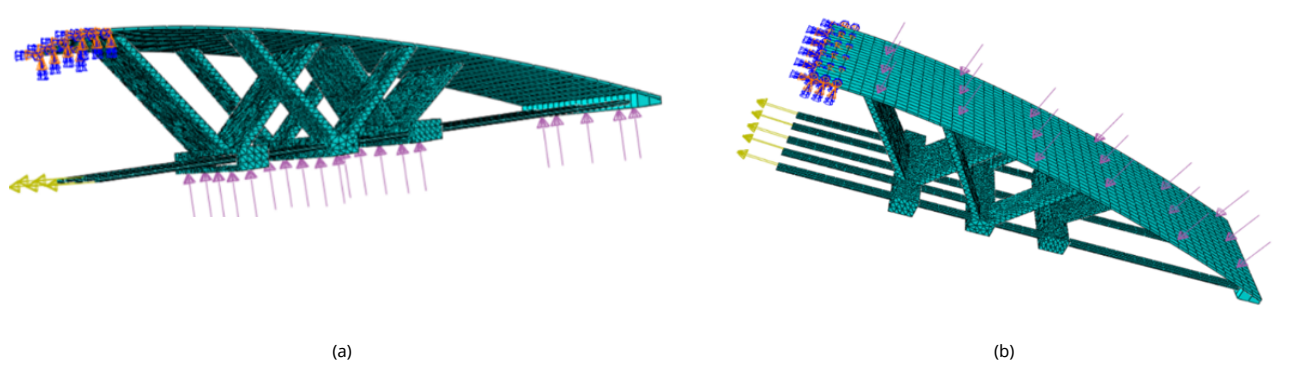

(a) (b)

Figure 11. Finite element model for load capacity analysis

3.2.1 Load-bearing capacity of applying pressure to the bottom of the truss

As shown in Figure 12, the maximum stress of the camber-morphing wing is 17280Pa, concentrated at the contact area between the deformable truss and the skin near the leading edge, while the stress at the contact area between the other deformable trusses and the skin is relatively small.

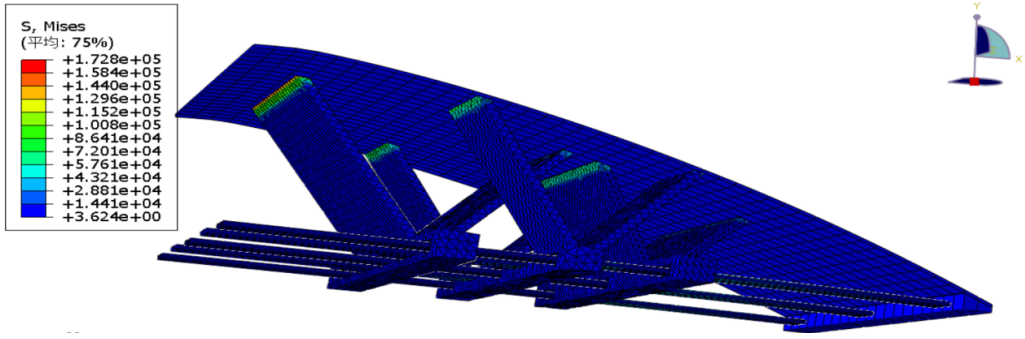

Figure 12. Stress when applying pressure to the bottom of the truss

As shown in Figure 13, when a concentrated force of 1000N is applied horizontally on the end of all metal wires, and a pressure is applied on the bottom of the deformable truss, the displacement of the wing tip is maximum, reaching 201.9mm. Due to the fixed connection between the upper edge of the skin and the leading edge, the upper edge of the skin is fixed, so there is almost no displacement in the front deformable truss near the leading edge. Due to the stress on the metal wire, the skin deforms, causing downward displacement of each deformable truss. The contact area between the groove of the truss and the metal wire will press down on the metal wire, causing it to bend. Meanwhile, there was no significant deformation in the entire structure.

3.2.2 Load-bearing capacity when applying pressure to the upper skin

As shown in Figure 14, when a concentrated force of 1000N is applied horizontally on the end of all metal wires and pressure is applied on the upper skin, the maximum stress of the camber-morphing wing is 17310Pa, which is concentrated at the contact area between the deformable truss and the skin near the leading edge. The stress at the contact area between the other deformable trusses and the skin is relatively small. At the same time, the metal wire passes through the deformable truss and contacts with it. When the skin makes the truss deflect downwards, the groove of the deformable truss will also apply downward pressure on the metal wire, causing slight bending of the metal wire. Therefore, there is also stress concentration at the contact area between the metal wire and the deformable truss. The overall stress conforms to the expected load of the camber-morphing wing model.

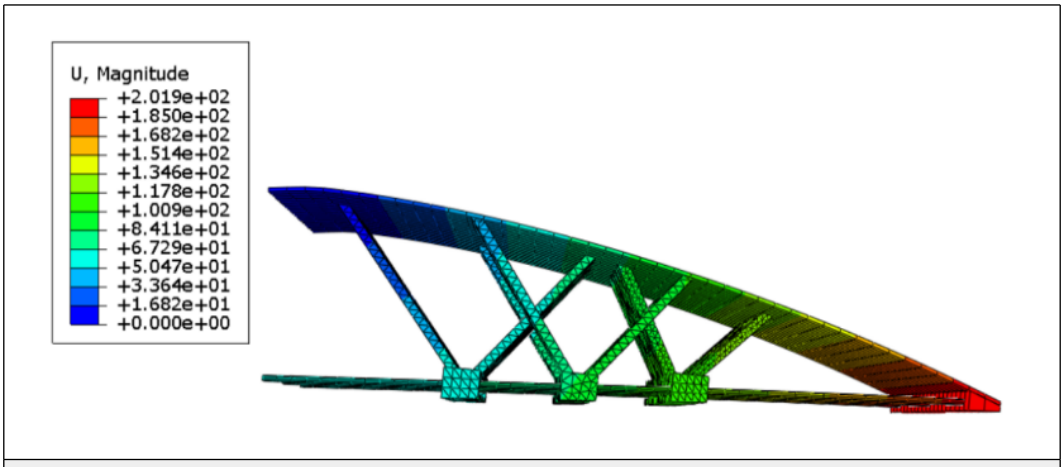

Figure 13. Displacement when applying pressure to the bottom of the truss

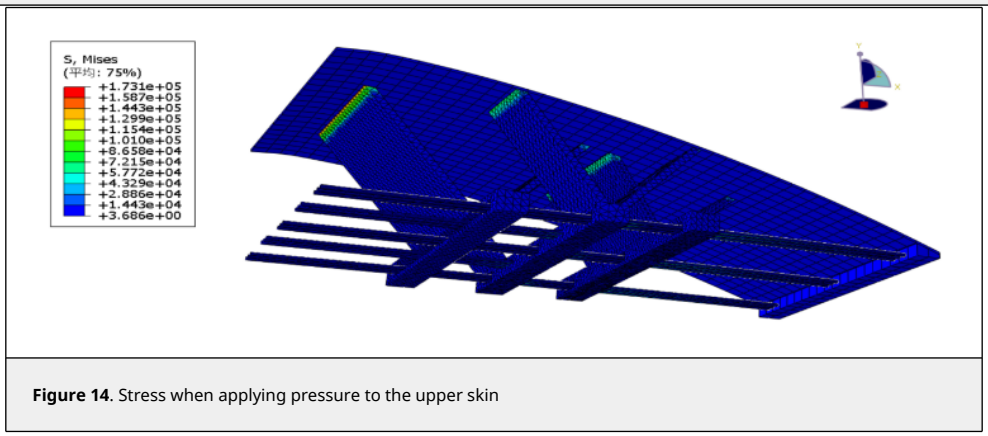

Figure 14. Stress when applying pressure to the upper skin

As shown in Figure 15, when a concentrated force of 1000N is applied horizontally on the end of all metal wires and pressure is applied on the surface of the skin, the displacement of the wing tip is the highest, reaching 204.4mm. Due to the fixed connection between the upper edge of the skin and the leading edge, the upper edge of the skin is fixed, so there is almost no displacement in front of the deformable truss near the leading edge. Due to the driving force on the metal wire, the skin deforms, causing downward displacement of each deformable truss. The contact area between the groove of the truss and the metal wire will press down on the metal wire, causing it to bend to a certain extent.

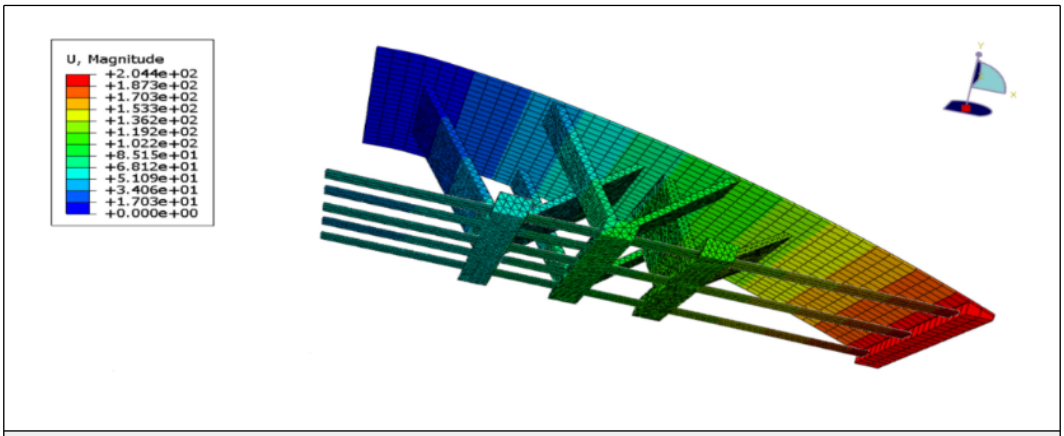

Figure 15. Displacement when applying pressure to the upper skin

Combining Sections 3.2.1 and 3.2.2, it can be seen that even with a decrease in structural stiffness, i.e. three sets of deformable trusses, regardless of whether pressure is applied to the lower edge of the truss or the upper skin, the

stress concentration is located at the connection between the skin and the truss, but it does not exceed the strength of the material. The displacement distribution also meets expectations. Therefore, it can withstand a certain external load.

4. Conclusions

A camber-morphing wing based on a deformable truss is proposed in this paper, in which the deformation mode of this wing is easier to manufacture and implement in engineering. Then, using the finite element method, the deformation and load-bearing capacity of the structure are verified, and the following conclusions can be drawn:

(1) Compared with the existing concept of camber-morphing wings, the deformation mode of this wing is easy to manufacture and implement in engineering;

(2) Due to its multiple degrees of freedom, the structure can achieve deformation under various driving conditions;

(3) Compared to driving short metal wires, driving long metal wires can achieve greater camber;

(4) An analysis of the load-bearing capacity of the wing structure revealed that it has sufficient stiffness to withstand certain external loads.

(5) From the current simulation results, it can be seen that the model has achieved downward deflection of the trailing edge, and further research is needed to determine whether the trailing edge can achieve upward deflection. Mainly because the current downward deflection of the camber-morphing trailing edge can increase the camber, which is conducive to the increase of lift, while the degree of upward deflection is not as great as that of downward deflection. So there is no further study on upward deflection in the simulation. Further research will be considered.

Funding: This research is supported by Natural Science Basic Research Plan in Shaanxi Province of China (2021JQ-847 and 2019JQ-912).

References

[1] Darecki M., Edelstenne C., Enders T., et al. Flightpath 2050: Europe's vision for aviation maintaining global leadership and serving society's needs. Publications Office of the European Union, Luxembourg, pp. 1-11, 2011.

[2] Ajaj R.M., Parancheerivilakkathil M.S., Amoozgar M.R., et al. Recent developments in the aeroelasticity of morphing aircraft. Progress in Aerospace Sciences, 120:1-29, 2021.

[3] Ajaj R.M., Beaverstock C.S., Michael I. Friswell. Morphing aircraft: the need for a new design philosophy. Aerospace and Technology, 49:154-166, 2016.

[4] Yang Y., Wang B.W., Lv S.S., et al. Review of technical development of variable camber wing (in Chinese). Acta Aeronautica et Astronautica Sinica, 43(1):24943-024943, 2020.

[5] Haughn K.P.T., Inman D.J. Spanwise camber morphing offers potential efficiency gains during autonomous gust rejection. AIAA SciTech 2024 Forum, Orlando, FL, USA, AIAA, pp. 1-8, 2024.

[6] Wu R., Soutis C., Zhong S., Filippone A. A morphing aerofoil with highly controllable aerodynamic performance. Aeronautical Journal, 121(1235):54-72, 2017.

[7] González A., Hinojosa J. Study of the influence of protuberances in the trailing edge of airfoils and determination of their aerodynamic efficiency through CFD using Ansys Fluent. Revista Internacional de Métodos Numéricos para Cálculo y Diseño en Ingeniería, 35(3), 36, 2019.

[8] Kota S., Hetrick J.A., Osborn R., Paul D., Pendleton E., Flick P., et al. Design and application of compliant mechanisms for morphing aircraft structures. Proceedings of SPIE Smart Structures and Materials 2003, 5054:24–33, August 2003.

[9] Hetrick J.A., Osborn R.F., Kota S., et al. Flight testing of mission adaptive compliant wing. 48th AIAA/ASME/ASCE/AHS/ASC Structures, Structural Dynamics, and Materials Conference, Honolulu, Hawaii, April 2007.

[10] Woods B.K., Bilgen O., Friswell M.I. Wind tunnel testing of the fish bone active camber morphing concept. Journal of Intelligent Material Systems and Structures, 25(7):772–85, 2014.

[11] Piet C.W., Padopoulos M. Smart intelligent aircraft structures (SARISTU). International Publishing, Springer Cham, 2015.

[12] Ni Y., Yang Y. Research on the status and key technology in morphing airfoil of adaptive wings (in Chinese). Advances in Aeronautical Science and Engineering, 9(3):297-308, 2018.

[13] Ni Y., Zhao H., Qiao S., et al. Development of aeroelastic modeling and analysis for wing camber morphing technology (in Chinese). Advances in Aeronautical Science and Engineering, 14(4):1-17, 2023.

[14] Campanile L.F., Sachau D. The belt-rib concept: A structronic approach to variable camber. Journal of Intelligent Material Systems and Structures, 11:215-224, 2000.

[15] Matteo N.D., Guo S., Morishingma R. Optimization of leading edge and flap with acturation system for a variable camber wing. 53rd AIAA/ASME/ASCE/AHS/ASC Structures, Structural Dynamics and Materials Conference, Honolulu, Hawaii, April 2012.

[16] Matteo N.D., Guo S., Ahmed S., et al. Morphing trailing edge flap for high lift wing. 52nd AIAA/ASME/ASCE/AHS/ASC Structures, Structural Dynamics and Materials Conference, Denver, Colorado, April 2011.

[17] Matteo N.D., Guo S., Ahmed S., et al. Design and analysis of a morphing flap structure for high lift wing. 51st AIAA/ASME/ASCE/AHS/ASC Structures, Structural Dynamics, and Materials Conference, Orlando, Florida, April 2010.

[18] Wang D.P., Bartley-Cho J.D., Martin C.A., et al. Development of high-rate, large deflection, hingeless trailing edge control surface for the smart wing wind tunnel model. Smart Applications of Smart Structures Technologies Proceedings of SPIE, 4332:407-418, 2001.

[19] Bartey-Cho J.D., Wang D.P., Martin C.A., et al. Development of hight-rate, adaptive trailing edge control surface for the smart wing phase 2 wind tunnel model. Journal of Intelligent Material Systems and Structures, 5(4):279-291, 2004.

[20] Zhang S., Yang Y., Wang Z., et al. Design and validation of eccentric beam for variable camber trailing edge (in Chinese). Acta Aeronautica et Astronautica Sinica, 43(6):525892, 2022.